

A theoretical study of cation– π interactions: Li^+ , Na^+ , K^+ , Be^{2+} , Mg^{2+} and Ca^{2+} complexation with mono- and bicyclic ring-fused benzene derivatives

Tandabany C. Dinadayalane · Ayorinde Hassan ·
Jerzy Leszczynski

Received: 3 June 2011 / Accepted: 18 August 2011 / Published online: 15 February 2012
© Springer-Verlag 2012

Abstract DFT (B3LYP functional) and MP2 methods using 6-311+G(2d,2p) basis set have been employed to examine the effect of ring fusion to benzene on the cation– π interactions involving alkali metal ions (Li^+ , Na^+ , and K^+) and alkaline earth metal ions (Be^{2+} , Mg^{2+} and Ca^{2+}). Our present study indicates that modification of benzene (π -electron source) by fusion of monocyclic or bicyclic (or mixture of these two kinds of rings) strengthens the binding affinity of both alkali and alkaline earth metal cations. The strength of interaction decreases in the following order: $\text{Be}^{2+} > \text{Mg}^{2+} > \text{Ca}^{2+} > \text{Li}^+ > \text{Na}^+ > \text{K}^+$ for any considered aromatic ligand. The interaction energies for the complexes formed by divalent cations are 4–6 times larger than those for the complexes involving monovalent cations. The structural changes in the ring wherein metal ion binds are examined. The distance between ring centroid and the metal ion is calculated for all of the complexes. Strained bicyclo[2.1.1]hexene ring fusion has substantially larger effect on the strength of cation– π interactions than the monocyclic ring fusion for all of the cations due to the π -electron localization at the central benzene ring.

Keywords Cation– π interactions · Ring-fused benzene · Density functional theory · Vibrational frequency · Extent of charge transfer

1 Introduction

Cation– π interactions are increasingly recognized in the fields of chemistry, biology and materials science [1–3]. They are proven to be important in protein structures [4–6], associations of biomolecules [7], the functioning of ion channels in membranes [8, 9], and ionophores [10]. Pletneva et al. based on their experimental results highlighted the role of cation– π interactions in both intermolecular recognition at the protein–protein interface and intramolecular processes like protein folding [7]. Cation– π interactions include electrostatic, inductive and charge transfer effects and, in some cases, dispersion forces [11]. Earlier studies have shown that the strength of cation– π interactions depends on the nature of both the π -system and the cation involved [12–14]. The strength of cation– π interactions of alkaline earth metal dication/benzene complexes is substantially stronger than alkali metal cation/benzene complexes [15]. Recently, Dinadayalane et al. have investigated $\text{C-H}\cdots\pi$, π – π and cation– π interactions involving benzene and large π -systems [16–22]. A theoretical study by Wheeler and Houk revealed that the substituent effects in cation– π interactions arise primarily from through-space effects of the substituents, and polarization of the benzene π system does not provide significant contribution toward this phenomenon [23]. The effect of substituents on cation– π interactions has been investigated by several groups [23–36].

Experimental and computational chemists have explored the cation– π interactions involving polycyclic and acyclic

Dedicated to Professor Eluvathingal D. Jemmis and published as part of the special collection of articles celebrating his 60th birthday.

Electronic supplementary material The online version of this article (doi:10.1007/s00214-012-1131-0) contains supplementary material, which is available to authorized users.

T. C. Dinadayalane (✉) · A. Hassan · J. Leszczynski (✉)
Department of Chemistry and Biochemistry, Interdisciplinary
Center for Nanotoxicity, Jackson State University,
1400 JR Lynch Street, P.O. Box 17910,
Jackson, MS 39217, USA
e-mail: dina@icnanotox.org

J. Leszczynski
e-mail: jerzy@icnanotox.org

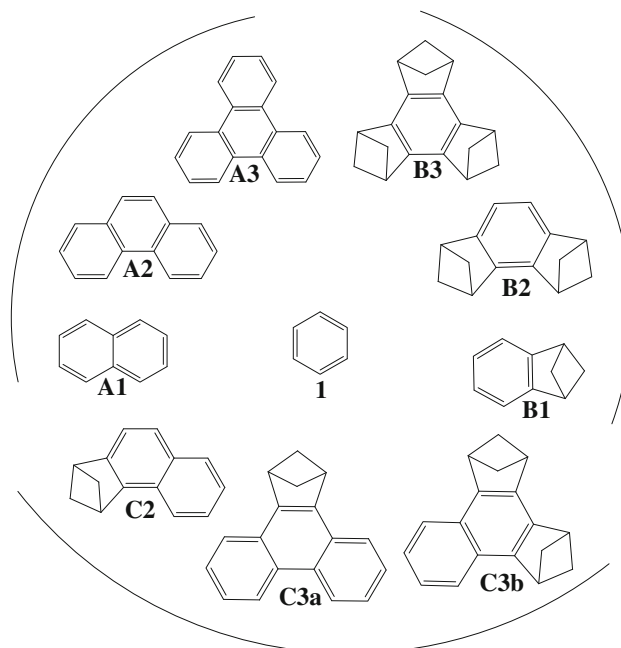
π -conjugated systems [37–39]. The current research interest is to understand the influence of cation– π interactions with other non-covalent forces such as hydrogen bonding and π – π interactions [1, 40–46]. Theoretical studies have shown the importance of multiple weak cation– π interactions in overall binding strength of the complexes involving cage or cup-like shaped ligands [17, 47]. Ring annelated benzene systems and curved polycyclic aromatic systems have been studied both experimentally and theoretically [48–58]. The cation– π interactions involving molecular bowls have stimulated recent theoretical interest [59, 60]. The polycyclic π -conjugated system, in which three pyrrole rings are fused to the alternate C–C bonds of benzene, has been considered for cation– π interactions in a recent theoretical study [44]. Density functional theory study has recently demonstrated the geometric effects and the orientation of π -electrons on the cation– π interactions [61]. Since different mono-, bis- and tris-annelated benzene systems were reported experimentally [48–54], we have explored the cation– π interactions involving ring-fused benzene systems using quantum chemical calculations in this paper. Understanding of the molecular-level details of cation– π interactions involving ring-fused benzene systems is crucial for designing of novel ionophores, molecular receptors and novel functional materials.

The present study is aimed to understand how the structural modifications of the π -electron system (i.e., benzene derivatives by ring fusion) affect the strength of cation– π interactions. We considered alkali (Li^+ , Na^+ and K^+) and alkaline earth (Be^{2+} , Ca^{2+} and Mg^{2+}) metal ions. The structures of benzene derivatives are considered as the fusion of mono- (i.e., benzene) and bicyclic (i.e., bicyclo[2.1.1]hexeno) rings to the C–C bonds of the benzene ring. One to three rings were fused with benzene. The structures of the benzene derivatives are depicted in Scheme 1. It is important to explain the nomenclature used here. The prototype benzene is numbered **1**, and **A** is used in designating monocyclic ring fusion to the alternate C–C bonds of benzene. The number followed by letter **A** represents the number of monocyclic ring fused to benzene. For example, system **A1** means a monocyclic ring is fused to benzene, while **A2** is used to denote two monocyclic rings fused to the central benzene. The numbering for **B** systems follows the same convention as discussed above, except **B** represents bicyclic ring fused to the benzene. The letter **C** is used to mention a mixture of both monocyclic and bicyclic rings fused to benzene. Results of our computational study will be useful to experimental chemists working in the area of cation– π interactions, particularly to uncover their molecular structures and interaction energies. It should be noted that many of the ligands considered here have already been synthesized. Our study may stimulate

experimental and theoretical interests on cation– π interactions involving large extended π -systems.

2 Computational details

All structures were optimized initially with the hybrid density functional theory method using B3LYP functional [62, 63] in conjunction with a 6-311+G(2d,2p) basis set. The aromatic systems and their metal ion complexes were confirmed as minima on their respective potential energy surfaces by carrying out harmonic vibrational frequency calculations. The optimized geometries were further relaxed with a second-order Moller–Plesset perturbation (MP2) method [64], with all electrons included in the correlation treatment employing the same basis set (i.e. level was employed). The interaction energies were corrected for basis set superposition error (BSSE) at both levels of theory using counterpoise technique proposed by Boys and Bernardi [65]. Mulliken and NPA charges obtained at the B3LYP/6-311G(d,p)//B3LYP/6-311+G(2d,2p) level were used in calculating the amount of charge transferred from the aromatic moieties to the cations, by subtracting the residual charge on the cation in the complex from its initial charge of +1 for alkali metal or +2 for alkaline earth metal cations. We encountered unrealistic values in NPA charges at the B3LYP/6-311+G(d,p) and B3LYP/6-311+G(2d,2p) levels for the cation– π interactions involving extended π -systems (see supplementary



Scheme 1 Structures of ligands considered for complexation with metal ions

material) [66]. The errors obtained here are due to linear dependence of basis functions. We have overcome the linear dependence condition by adding IOP(6/76 = 8) keyword [67]. In order to avoid ambiguity in charge analysis, we removed diffuse functions and uniformly performed NPA calculations at the B3LYP/6-311G(d,p) level, and these results are used for discussion in this paper. The NPA charges were calculated using NBO 3.1 [68] implemented in Gaussian 09 software [69]. All calculations were performed using Gaussian 09 program package [69]. Molecular electrostatic potential (MESP) surfaces were generated for the ligands considered in the study using the electron density obtained at the MP2(FULL)/6-311+G(2d,2p) level. Gaussview 3.0 was used in generating the pictures of MESP surfaces [70].

3 Results and discussion

3.1 Equilibrium geometries

All geometries obtained at the B3LYP/6-311+G(2d,2p) level are confirmed to be true energy minima by virtue of

not possessing any imaginary frequency. However, the harmonic vibrational frequency calculations were not performed at the MP2(FULL)/6-311+G(2d,2p) level due to the computational cost. Key structural parameters for the ligands and their metal-ion-bound complexes at both levels are given in Figs. 1, 2 and 3. Large structural changes should occur at the central benzene ring where the metal ion binds. Therefore, we provide the C–C bond distances of the central benzene ring for the ligands and their complexes in Figs. 1, 2 and 3. A perusal of the geometrical data provided in Figs. 1, 2 and 3 indicates that the majority of bond distances obtained at the B3LYP and MP2 levels are comparable. The notable exception is the **B3** system and its complexes where the B3LYP overestimates the bond lengths compared to MP2 method.

It should be noted that the distance between K^+ and center of the π -ring, where the metal ion binds, is always longer at the B3LYP than at the MP2 for all the complexes formed with K^+ . The deviation of the above-mentioned distance between these two theory levels ranges from 0.05 to 0.1 Å. The interaction energy for the benzene- K^+ complex (**1-K⁺**) at the MP2(FULL)/6-311+G(2d,2p) level

Fig. 1 Selected bond distances for the ligands of planar aromatic systems (**1**, **A1**, **A2** and **A3**) and their complexes formed by the metal ion binding. The distance between the metal ion and the center of central six-membered ring of the ligand, R_{CM} , is also given for all complexes. The values given in *plain* and *bold* correspond to the B3LYP/6-311+G(2d,2p) and MP2(FULL)/6-311+G(2d,2p) levels, respectively. All values are in Å

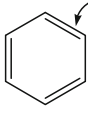
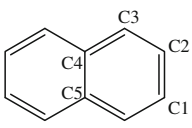
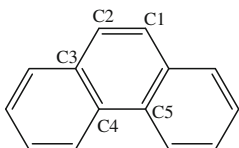
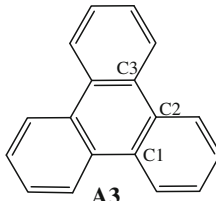
 <p>1</p>						
			R_{CM}	M		
			1.392 (1.394)			
			1.400 (1.401)	1.841 (1.845)	Li ⁺	
			1.398 (1.400)	2.392 (2.391)	Na ⁺	
			1.396 (1.398)	2.880 (2.823)	K ⁺	
 <p>A1</p>						
					R_{CM}	M
			C1–C2	C2–C3	C3–C4	C4–C5
			1.413 (1.412)	1.372 (1.377)	1.417 (1.415)	1.428 (1.429)
			1.419 (1.418)	1.381 (1.385)	1.424 (1.423)	1.438 (1.439)
			1.419 (1.417)	1.378 (1.383)	1.424 (1.421)	1.436 (1.437)
 <p>A2</p>						
					R_{CM}	M
			C1–C2	C2–C3	C3–C4	C4–C5
			1.354 (1.362)	1.432 (1.428)	1.422 (1.423)	1.455 (1.446)
			1.365 (1.371)	1.438 (1.434)	1.431 (1.431)	1.462 (1.455)
			1.361 (1.368)	1.438 (1.433)	1.428 (1.429)	1.462 (1.453)
 <p>A3</p>						
					R_{CM}	M
			C1–C2	C2–C3		
			1.416 (1.417)	1.464 (1.456)		
			1.424 (1.425)	1.471 (1.463)	1.803 (1.810)	Li ⁺
			1.422 (1.423)	1.471 (1.462)	2.334 (2.322)	Na ⁺

Fig. 2 Selected bond distances for the ligands of bicyclo[2.2.1]hexene ring-fused benzene systems (**B1**, **B2** and **B3**) and their complexes formed by the metal ion binding. The distance between the metal ion and the center of central six-membered ring of the ligand, R_{CM} , is also given for all complexes. The values given in *plain* and *bold* correspond to the B3LYP/6-311+G(2d,2p) and MP2(FULL)/6-311+G(2d,2p) levels, respectively. All values are in Å

bond distances

ene ring-fused
(**B1**, **B2** and
complexes formed
binding. The
the metal ion
central six-
f the ligand,
n for all
values given in
respond to the
(2d,2p) and
1+G(2d,2p)
ly. All values

B1

C1–C2	C2–C3	C3–C4	C4–C5	R_{CM}	M
1.388 (1.395)	1.406 (1.404)	1.376 (1.381)	1.408 (1.405)		
1.395 (1.402)	1.415 (1.412)	1.385 (1.389)	1.419 (1.417)	1.808 (1.811)	Li ⁺
1.393 (1.400)	1.414 (1.410)	1.382 (1.388)	1.417 (1.414)	2.363 (2.358)	Na ⁺
1.392 (1.399)	1.411 (1.409)	1.381 (1.386)	1.414 (1.411)	2.844 (2.776)	K ⁺
1.412 (1.418)	1.434 (1.432)	1.405 (1.408)	1.447 (1.444)	1.270 (1.276)	Be ²⁺
1.405 (1.411)	1.429 (1.425)	1.398 (1.402)	1.439 (1.435)	1.897 (1.906)	Mg ²⁺
1.400 (1.406)	1.419 (1.416)	1.389 (1.394)	1.429 (1.424)	2.315 (2.309)	Ca ²⁺

B2

C1–C2	C2–C3	C3–C4	C4–C5	R_{CM}	M
1.421 (1.414)	1.372 (1.382)	1.422 (1.415)	1.362 (1.371)		
1.431 (1.423)	1.381 (1.389)	1.434 (1.426)	1.372 (1.379)	1.780 (1.783)	Li ⁺
1.430 (1.422)	1.378 (1.388)	1.432 (1.423)	1.369 (1.377)	2.337 (2.331)	Na ⁺
1.427 (1.419)	1.376 (1.386)	1.429 (1.421)	1.367 (1.375)	2.817 (2.738)	K ⁺
1.450 (1.445)	1.400 (1.406)	1.460 (1.455)	1.394 (1.398)	1.246 (1.254)	Be ²⁺
1.446 (1.437)	1.392 (1.400)	1.454 (1.444)	1.386 (1.392)	1.877 (1.883)	Mg ²⁺
1.434 (1.427)	1.385 (1.393)	1.442 (1.433)	1.376 (1.383)	2.280 (2.273)	Ca ²⁺

B3

C1–C2	C2–C3	R_{CM}	M
1.437 (1.426)	1.358 (1.369)		
1.450 (1.437)	1.368 (1.378)	1.754 (1.757)	Li ⁺
1.449 (1.435)	1.365 (1.376)	2.308 (2.303)	Na ⁺
1.445 (1.431)	1.363 (1.375)	2.781 (2.704)	K ⁺
1.477 (1.468)	1.388 (1.395)	1.219 (1.233)	Be ²⁺
1.471 (1.456)	1.380 (1.390)	1.857 (1.866)	Mg ²⁺
1.456 (1.443)	1.372 (1.381)	2.252 (2.244)	Ca ²⁺

C2

C1–C2	C2–C3	C3–C4	C4–C5	C5–C6	C1–C6	R_{CM}	M
1.383 (1.386)	1.396 (1.397)	1.385 (1.389)	1.402 (1.401)	1.440 (1.440)	1.415 (1.416)		
1.393 (1.395)	1.402 (1.404)	1.398 (1.400)	1.411 (1.410)	1.449 (1.448)	1.423 (1.425)	1.795 (1.798)	Li ⁺
1.390 (1.392)	1.402 (1.403)	1.393 (1.396)	1.410 (1.408)	1.448 (1.447)	1.421 (1.423)	2.347 (2.344)	Na ⁺
1.388 (1.390)	1.399 (1.401)	1.391 (1.395)	1.407 (1.406)	1.445 (1.445)	1.419 (1.421)	2.829 (2.759)	K ⁺
1.413 (1.413)	1.419 (1.423)	1.426 (1.426)	1.429 (1.430)	1.476 (1.475)	1.441 (1.445)	1.243 (1.248)	Be ²⁺
1.404 (1.405)	1.419 (1.419)	1.417 (1.417)	1.428 (1.426)	1.468 (1.467)	1.437 (1.438)	1.863 (1.868)	Mg ²⁺
1.396 (1.398)	1.407 (1.409)	1.405 (1.405)	1.417 (1.415)	1.457 (1.456)	1.429 (1.430)	2.264 (2.256)	Ca ²⁺

C3a

C1–C2	C2–C3	C3–C4	C4–C5	R_{CM}	M
1.365 (1.375)	1.417 (1.411)	1.431 (1.433)	1.456 (1.449)		
1.378 (1.385)	1.425 (1.419)	1.440 (1.441)	1.464 (1.458)	1.788 (1.794)	Li ⁺
1.373 (1.382)	1.424 (1.418)	1.438 (1.439)	1.463 (1.456)	2.338 (2.331)	Na ⁺
1.371 (1.380)	1.421 (1.415)	1.436 (1.437)	1.461 (1.453)	2.823 (2.725)	K ⁺
1.407 (1.409)	1.441 (1.439)	1.463 (1.465)	1.486 (1.484)	1.212 (1.220)	Be ²⁺
1.398 (1.402)	1.443 (1.436)	1.454 (1.455)	1.483 (1.476)	1.835 (1.839)	Mg ²⁺
1.385 (1.390)	1.429 (1.423)	1.445 (1.446)	1.471 (1.465)	2.224 (2.215)	Ca ²⁺

C3b

C1–C2	C2–C3	C3–C4	C4–C5	R_{CM}	M
1.380 (1.385)	1.397 (1.397)	1.399 (1.403)	1.452 (1.450)		
1.388 (1.393)	1.410 (1.408)	1.408 (1.412)	1.461 (1.458)	1.769 (1.775)	Li ⁺
1.387 (1.392)	1.406 (1.404)	1.406 (1.410)	1.460 (1.457)	2.327 (2.325)	Na ⁺
1.384 (1.389)	1.402 (1.403)	1.404 (1.408)	1.458 (1.455)	2.827 (2.737)	K ⁺
1.407 (1.412)	1.437 (1.434)	1.428 (1.432)	1.487 (1.484)	1.223 (1.232)	Be ²⁺
1.406 (1.409)	1.427 (1.423)	1.424 (1.427)	1.479 (1.475)	1.851 (1.856)	Mg ²⁺
1.392 (1.396)	1.415 (1.412)	1.414 (1.417)	1.467 (1.464)	2.224 (2.231)	Ca ²⁺

Fig. 3 Selected bond distances for the ligands of both benzene and bicyclo[2.2.1]hexene ring-fused benzene systems (**C2**, **C3a** and **C3b**) and their complexes formed by the metal ion binding. The distance between the metal ion and the center of central six-membered ring of

the ligand, R_{CM} , is also given for all complexes. The values given in *plain* and *bold* correspond to the B3LYP/6-311+G(2d,2p) and MP2(FULL)/6-311+G(2d,2p) levels, respectively. All values are in Å

is in very good agreement with the experimental value, while the interaction energy at the B3LYP/6-311+G(2d,2p) level is slightly lower than the experimental result. A combined experimental and theoretical study also

reported that MP2(FULL)/6-311+G(2d,2p) level provides much better correlation between the theoretical and experimental results for cation– π interaction energies than the B3LYP/6-311+G(2d,2p) level [38]. Therefore, for the

consistency, the geometrical parameters and interaction energies obtained at the MP2(FULL)/6-311+G(2d,2p) level are taken for discussion in this paper unless otherwise stated. Some features of the bond lengths of some of the complexes have been previously reported by us but only at the B3LYP/6-31G(d,p) level. We have shown in our earlier studies that when the ring-fused π -system is highly symmetric (i.e., mono- or bicyclic rings are fused to three alternate C–C bonds of benzene), the cation resides directly above the center of the ring; otherwise, the cation is slightly displaced from the center [16, 18]. The same situation is observed here in complexes involving both alkali and alkaline earth metal cations.

Some interesting conclusions can be extracted from the geometrical results. The distance between metal cation and the ring centroid, R_{CM} , in the complexes is shown to constantly increase as the ionic radius of the cation increases, for both the monovalent and divalent cations. Thus, the complexes of smaller cations, Li^+ and Be^{2+} , have shorter R_{CM} than their monovalent and divalent counterparts, respectively. As the number of fused rings increases, the distance R_{CM} decreases for the complexes of each metal ion. The extent of this decrease is more pronounced for the bicyclic systems in comparison with their corresponding monocyclic systems when alkali metals are considered. Thus, for a given alkali metal ion, **B1**, **B2** and **B3** complexes exhibit shorter R_{CM} distances than **A1**, **A2** and **A3** complexes, respectively. Conversely, this trend is reversed when the alkaline earth metals are being examined; the bicyclic systems display longer R_{CM} distances than the monocyclic counterparts (Figs. 1 and 2). This may be ascribed to repulsion between the dication and the positively charged hydrogen (bridge CH_2) of the fused ring of bicyclo[2.1.1]hexene framework in **B1**, **B2** and **B3**. It is worth mentioning that regardless of which π -system is considered, Be^{2+} complexes consistently have the shortest R_{CM} . The complexes formed with divalent cations exhibit shorter R_{CM} distances than the complexes involving Na^+ and K^+ .

The C–C bonds of the central six-membered rings of the π -systems are elongated upon metal ion binding as shown in Figs. 1, 2 and 3. The degree of elongation of the bonds is much higher for the binding of alkaline earth metal ions than the alkali metal ions. Binding of Li^+ and Be^{2+} elongates the C–C bonds of the central ring of π -system to the maximum extent in alkali and alkaline earth metal cation– π complexes, respectively. In all cases, Be^{2+} complexation elongates and weakens the C–C bond lengths of the ligands to the most extent. Benzene (**1**) has equal lengths for all C–C bonds, but ring fusion to benzene generates different C–C bond lengths. The number of C–C bond lengths in complexes is same as in the corresponding ligand.

Investigations of aromatic characters of localized (or bond alternate) benzene derivatives are of current interest [71, 72]. Frank et al. revealed that trisbicyclo[2.1.1]heptabenzene (**B3**) is a very good example for strain-induced bond alternation in benzenoid aromatics. They reported ~ 0.06 Å difference between the endo and exo bond lengths at the MP2/6-31G(d) level [50]. The value remains the same even at higher level calculations. This value is unaltered by complexation involving alkali metal ions, while it is slightly increased by alkaline earth metal ion complexation with **B3**. The difference in bond lengths between C1–C2 and C2–C3 is 0.04 Å for **A3** and its complexes.

The length of C–C bond shared by two six-membered rings increases as we move from **A1** to **A3**. The same trend is maintained in case of **B1**–**B3**. The metal ion binding does not affect this trend. Since the systems **A3**, **B3**, **C3a** and **C3b** are tris-annulated, we compare their structural features here. For a specific metal ion, the R_{CM} in **C3a**, and **C3b** is longer than in **B3** but it is shorter than in **A3**. However, the R_{CM} value given for **C3b** is shorter than that for **C3a** due to the effect of replacement of a monocyclic ring with a strained bicyclic ring. The present study reveals that the fusion of strained bicyclic ring to benzene has a considerable effect on the geometries of cation– π complexes.

3.2 Interaction energies, extent of charge transfer and molecular electrostatic potential

The BSSE corrected interaction energies for all of the complexes are provided in Table 1 along with the values of π -cloud thickness. Each carbon of central six-membered ring of ligands considered has 2p electrons; each carbon donates an electron into the delocalized ring above and below the benzene ring. It is the side-on overlap of p-orbitals that produces the π -clouds. The π -cloud thickness is defined as the distance between the plane of six-membered ring and the edge of π -cloud above or below the ring. The side in which the metal ion binds is considered for calculating the values of π -cloud thickness. As reported in earlier study [73], the π -cloud thickness was calculated by subtracting the radii of different cations [74] from the R_{CM} . The values of π -cloud thickness indicate the ability to which each cation can polarize the aromatic ligands. They decrease as increasing the number of fused rings for the complexes of each metal ion.

The values of interaction energies, correction for BSSE and BSSE corrected interaction energies obtained at two different levels considered are given in supplementary material. Figure 4 shows that the correction to BSSE is smaller at the B3LYP/6-311+G(2d,2p) level (less than 1 kcal/mol) than the MP2/6-311+G(2d,2p) level

Table 1 BSSE corrected interaction energies (ΔE , in kcal/mol) obtained at the B3LYP/6-311+G(2d,2p) and MP2(FULL)/6-311+G(2d,2p) (given in parentheses) levels along with the values of π -cloud thickness (in Å) calculated at the MP2(FULL)/6-311+G(2d,2p) level

System	Li ⁺	Na ⁺	K ⁺	Be ²⁺	Mg ²⁺	Ca ²⁺
1						
ΔE	−38.4 (−36.3)	−24.0 (−22.8)	−16.0 (−17.8)	−229.6 (−219.2)	−120.0 (−112.8)	−81.3 (−76.3)
Expt ^a	−38.5 ± 3.2	−22.1 ± 1.4	−17.5 ± 1.0	NA	NA	NA
π -cloud thickness	1.24	1.44	1.55	0.98	1.28	1.37
A1						
ΔE	−41.0 (−38.8)	−25.8 (−25.1)	−18.0 (−20.5)	−252.1 (−240.6)	−136.4 (−128.6)	−95.6 (−90.2)
Expt ^b	−44.7 ± 3.9	−25.6 ± 1.2	−19.3 ± 1.2	NA	NA	NA
π -cloud thickness	1.22	1.42	1.51	0.95	1.23	1.30
A2						
ΔE	−41.9 (−39.9)	−27.2 (−26.7)	−19.5 (−22.4)	−265.3 (−253.8)	−147.5 (−139.8)	−105.9 (−100.6)
π -cloud thickness	1.21	1.40	1.49	0.91	1.18	1.25
A3						
ΔE	−42.2 (−40.5)	−28.3 (−28.0)	−20.6 (−24.1)	−273.4 (−262.3)	−155.5 (−148.0)	−113.1 (−108.4)
π -cloud thickness	1.20	1.38	1.47	0.88	1.15	1.21
B1						
ΔE	−45.0 (−42.6)	−28.2 (−27.1)	−19.4 (−21.5)	−259.5 (−247.5)	−141.6 (−133.3)	−98.8 (−93.1)
π -cloud thickness	1.21	1.41	1.51	0.96	1.25	1.33
B2						
ΔE	−50.2 (−47.8)	−31.8 (−30.7)	−21.9 (−24.5)	−283.3 (−271.0)	−159.3 (−150.5)	−113.3 (−107.4)
π -cloud thickness	1.18	1.39	1.49	0.94	1.23	1.29
B3						
ΔE	−54.5 (−52.2)	−34.6 (−33.6)	−23.8 (−27.0)	−303.1 (−291.2)	−173.9 (−165.3)	−125.5 (−119.8)
π -cloud thickness	1.15	1.36	1.45	0.91	1.21	1.26
C2						
ΔE	−46.0 (−43.6)	−29.3 (−28.5)	−20.6 (−23.5)	−274.7 (−262.3)	−153.0 (−144.7)	−109.2 (−103.6)
π -cloud thickness	1.20	1.40	1.50	0.93	1.21	1.27
C3a						
ΔE	−45.9 (−43.9)	−29.9 (−29.5)	−21.4 (−25.0)	−283.5 (−271.7)	−161.1 (−153.2)	−116.9 (−111.8)
π -cloud thickness	1.19	1.39	1.49	0.90	1.19	1.23
C3b						
ΔE	−50.1 (−47.8)	−32.0 (−31.3)	−22.7 (−26.0)	−293.6 (−281.0)	−166.8 (−158.5)	−120.9 (−115.3)
π -cloud thickness	1.17	1.38	1.50	0.91	1.20	1.23

NA not available

^a Experimental ΔH values taken from Ref. [75]^b Experimental values taken from Ref. [38]

(1.2–5.0 kcal/mol). At the latter level, the BSSE correction increases as the number of fused rings increases. The interaction energies of all cation– π complexes are large and negative, indicating a favorable interaction. The computed interaction energies for **1**–Li⁺, **1**–Na⁺ and **1**–K⁺ are −36.3, −22.8 and −17.8 kcal/mol, which are in very good agreement with the experimental values of -38.5 ± 3.2 , -22.2 ± 1.4 and -17.5 ± 0.9 kcal/mol, respectively [75]. The interaction energies calculated for the binding of alkali metal ions with naphthalene (**A1**) at both levels are in close agreement with the reported experimental values [38]. For

each ligand, Be²⁺ binds much stronger than other divalent cations, while Li⁺ interaction is the strongest among the monovalent cations. This trend follows the R_{CM} distances corresponding to the complexes involving divalent and monovalent cations. As the ionic radius increases from Be²⁺ to Ca²⁺, the interaction energy for cation– π complexes decreases; the same situation is observed in case of alkali metal ion complexes (Fig. 5). Irrespective of the number or the type of rings fused to benzene (we mean any π -system considered in this study), the strength of Be²⁺ interaction is the strongest among all cations considered.

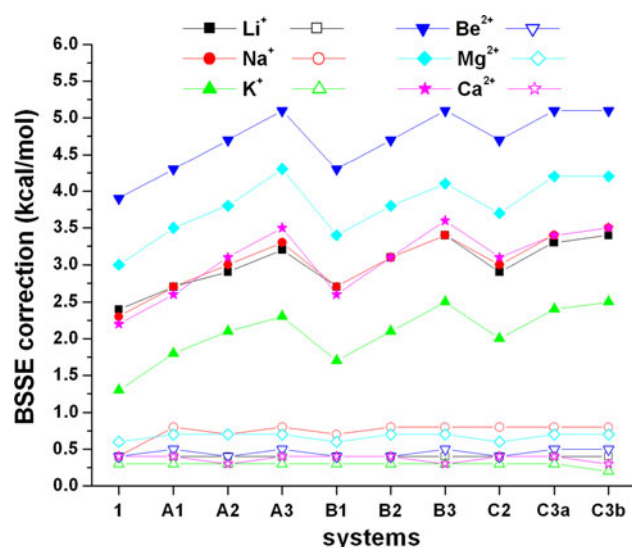


Fig. 4 The values of basis set superposition error correction (BSSE correction, kcal/mol) obtained at the MP2(FULL)/6-311+G(2d,2p) (given in *closed symbols*) and the B3LYP/6-311+G(2d,2p) (given in *open symbols*) levels for all complexes considered

As shown in Fig. 5, the strength of interaction decreases in the following order: $\text{Be}^{2+} > \text{Mg}^{2+} > \text{Ca}^{2+} > \text{Li}^+ > \text{Na}^+ > \text{K}^+$ for any given aromatic ligand.

The interaction energies for the complexes formed by divalent cations are substantially larger than that for the complexes involving monovalent cations. The binding strengths for the complexes of Be^{2+} , Mg^{2+} and Ca^{2+} are about 6, 5 and 4 times that of Li^+ , Na^+ and K^+ , respectively. The interaction energies for the former set of complexes approach those of typical chemical bonds, especially for the complexes of Be^{2+} and Mg^{2+} , where the energies are as high as -291 and -165 kcal/mol. The interaction energy data suggest that the nature of divalent

cation complexation with ligands could be different from monovalent ones, and the forces other than electrostatics may play vital role in stabilizing these complexes. Such high interaction energies were reported earlier for the alkaline earth metal ion binding with the aromatics [76, 77]. The interaction energies for the complexes between alkali metal ions and each ligand are similar to the strength of typical intermolecular interactions.

Electron-donating or electron-withdrawing substituent attached to benzene plays a role in cation- π interactions [23, 77]. Electron-withdrawing substituent to benzene weakens the binding strength of cation- π interactions, while electron-donating substituent to benzene makes cation- π interaction much stronger than the prototype benzene system [77]. Our present study indicates that modification of benzene (π -electron source) by fusion of monocyclic or bicyclic or mixture of these two kinds of rings strengthens the binding affinity of both alkali and alkaline earth metal cations. Furthermore, strained bicyclo[2.1.1]hexene ring fusion has substantially larger effect on the strength of cation- π interactions than the monocyclic ring fusion for all of the cations. This can be attributed to the π -electron localization at the central benzene ring as evidenced from the molecular electrostatic potential maps depicted in Fig. 6.

As shown in Fig. 5 and data provided in Table 1, increasing the number of ring fusion to benzene, irrespective of monocyclic or bicyclic ring fusion, progressively increases the binding affinity toward metal ions. For example, **B1**, **B2** and **B3** systems exhibit about 28, 50 and 72 kcal/mol larger interaction energies than **1** in case of Be^{2+} ion complexation. The binding strengths of Be^{2+} , Mg^{2+} and Ca^{2+} interactions with **B3** are enhanced correspondingly by 33, 46 and 58% compared to that of their respective interactions with **1**. Although, their interactions

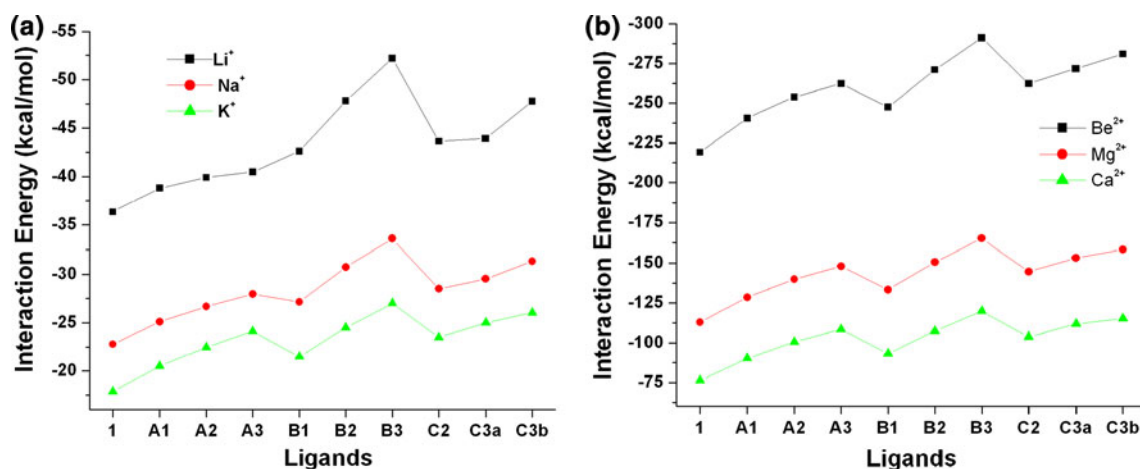


Fig. 5 Variation of interaction energies (kcal/mol) obtained at the MP2(FULL)/6-311+G(2d,2p) level for binding of alkali (a) and alkaline (b) earth metal cations with different ligands

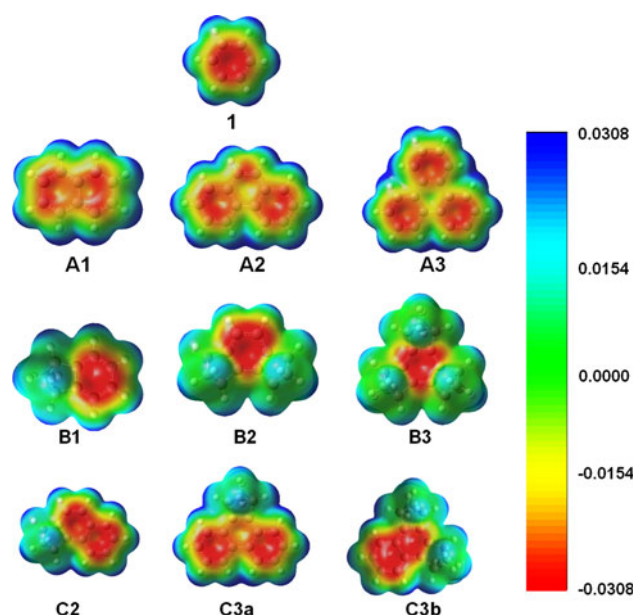


Fig. 6 Molecular electrostatic potential maps generated with MP2(FULL)/6-311+G(2d,2p) level electron density for all ligands considered in this study. Electrostatic potentials are mapped on the surface of the electron density of 0.002 unit. The *red* surface corresponds to a negative region of the electrostatic potential (-0.0308 au), whereas the *blue color* corresponds to the region where the potential is positive ($+0.0308$ au)

with **A3** are enhanced, the fraction of increased binding strength is lower (20, 31 and 42% correspondingly for Be^{2+} , Mg^{2+} and Ca^{2+} binding). Our study reveals that Li^+ ion is greatly benefited by strained bicyclo[2.1.1]hexene ring fusion to benzene compared to Be^{2+} . This is evidenced by more percentage increase in binding strength of Li^+ (17, 32 and 44%) than Be^{2+} (13, 23 and 33%) with the **B1**, **B2** and **B3**. The percentage increase in binding strength is calculated with respect to the corresponding metal ion–benzene complexes. Na^+ and Mg^{2+} ions have comparable percentage increase in binding strength with the above-mentioned ligands, while Ca^{2+} shows larger percentage increase in binding strength than K^+ . The large size of K^+ ion may prevent the effective cation– π interactions with the strained bicyclo[2.1.1]hexene ring-fused benzene systems.

For smaller monocations (Li^+ and Na^+), single bicyclic ring-fused benzene (**B1**) has slightly stronger binding affinity than two monocyclic ring-fused benzene (**A2**). This situation is not observed for other cations. It should be noted that Li^+ has stronger interaction with **C2** than **A3**, while both these ligands have almost equal binding strength in case of Be^{2+} . Except for Ca^{2+} ion, ligand **B2** is better than **A3** for cation binding. The cation binding ability of ligand **C2**, which has one six-membered and one bicyclic ring fused with benzene, is compared to that of **A1** and **B1**. For all cations considered, **C2** shows superior binding affinity than **A1** and **B1**. Although it is better than

A2 for cation binding, it is surpassed by **B2**. It is meaningful to compare the binding abilities of **A3**, **B3**, **C3a** and **C3b** since these ligands are tris-annulated benzene systems. Among these four ligands, **B3** is the most preferred and **A3** is the least preferred for metal ion binding; the binding ability of ligands for the metal ions decreases in the following order **B3**>**C3b**>**C3a**>**A3**. The interaction energy increases as the number of bicyclic ring annelation is increased with the complexes having the strongest interaction energies when the benzene is fully surrounded by bicyclic rings. Thus, the rigid bicyclic σ -framework, bicyclo[2.1.1]hexene fused to benzene, has significant impact on the cation– π interactions. From the pictures of molecular electrostatic potentials given in Fig. 6, one can see the increase in electron density in the central ring on going from **A3** to **C3a**, to **C3b**, and then to **B3**.

The data provided in Table 2 indicate that the electron charge transfer (q_{CT}) takes place from ligand to metal ion in the considered complexes. Figure 7 and Table 2 show, in general, the same qualitative trend for q_{CT} calculated using Mulliken and NPA charges. However, the magnitude of NPA charges is lower than Mulliken charges. Expectedly, the values of extent of charge transfer decrease as the metal ion size increases independently in alkali and alkaline earth metal–type complexes. As the number of fused rings to benzene increases, the charge transfer from ligand to metal ion also increases. In accordance with the interaction energies, the highest charge transfer takes place from **B3** to metal ions. Furthermore, **B1**, **B2** and **B3** complexes exhibit more charge transfer than **A1**, **A2** and **A3** complexes, respectively. Except for the alkali metal ion complexes with the **A1**–**A3** ligands, all other complexes of metal ions with ring-fused systems exhibit larger charge transfer values compared to the corresponding metal ion complex with the benzene.

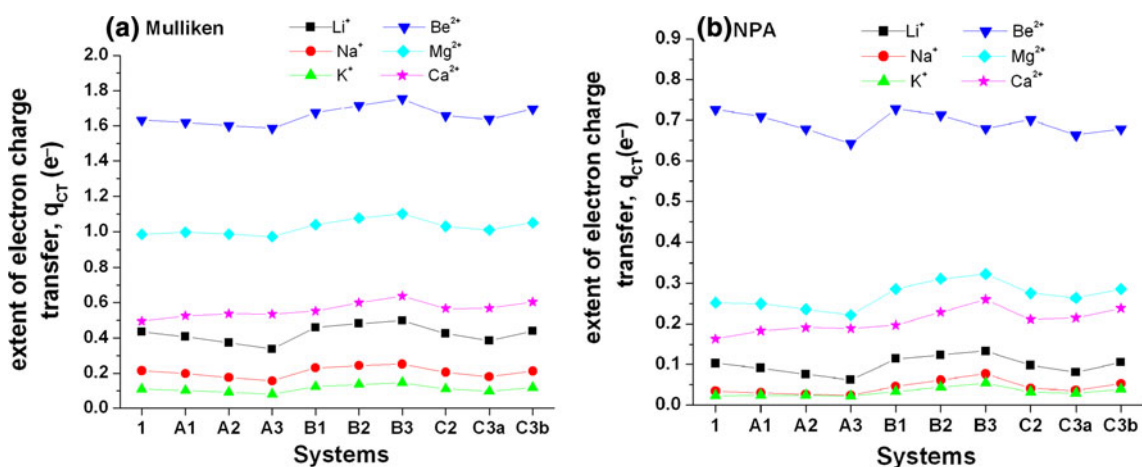
4 Conclusions

The results of calculations performed at both B3LYP and MP2 levels of theory clearly show that nature of the metal ion as well as the nature of the π -ligand does affect the binding strength of cation– π interactions. Increasing the number of ring fusion to benzene, irrespective of monocyclic or bicyclic ring fusion, increases the binding affinity toward metal ions. The rigid bicyclic σ -framework, bicyclo[2.1.1]hexene fusion to benzene, has significant effect on the geometries and the binding strength of cation– π interactions. Among the four ligands of tris-annulated benzene, the binding ability of ligands for the metal ions decreases in the following order **B3** > **C3b** > **C3a** > **A3**. For a given alkali metal ion, **B1**, **B2**, and **B3** complexes exhibit shorter R_{CM} distances than **A1**, **A2**, and **A3**

Table 2 The extent of charge transfer from ligand to metal ions (q_{CT} , e^-) obtained at the B3LYP/6-311G(d,p) level using Mulliken and natural population analysis

System	q_{CT} —Mulliken	q_{CT} —NPA	System	q_{CT} —Mulliken	q_{CT} —NPA
1-Li⁺	0.351	0.097	B2-Li⁺	0.389	0.119
1-Na⁺	0.211	0.033	B2-Na⁺	0.237	0.062
1-K⁺	0.150	0.030	B2-K⁺	0.187	0.052
1-Be²⁺	1.297	0.702	B2-Be²⁺	1.332	0.687
1-Mg²⁺	0.714	0.230	B2-Mg²⁺	0.805	0.294
1-Ca²⁺	0.538	0.203	B2-Ca²⁺	0.653	0.297
A1-Li⁺	0.339	0.086	B3-Li⁺	0.382	0.131
A1-Na⁺	0.198	0.030	B3-Na⁺	0.237	0.079
A1-K⁺	0.144	0.032	B3-K⁺	0.200	0.062
A1-Be²⁺	1.286	0.687	B3-Be²⁺	1.333	0.653
A1-Mg²⁺	0.731	0.230	B3-Mg²⁺	0.827	0.310
A1-Ca²⁺	0.572	0.240	B3-Ca²⁺	0.690	0.349
A2-Li⁺	0.315	0.073	C2-Li⁺	0.318	0.079
A2-Na⁺	0.181	0.027	C2-Na⁺	0.184	0.038
A2-K⁺	0.136	0.032	C2-K⁺	0.146	0.039
A2-Be²⁺	1.263	0.656	C2-Be²⁺	1.268	0.641
A2-Mg²⁺	0.730	0.219	C2-Mg²⁺	0.759	0.252
A2-Ca²⁺	0.588	0.264	C2-Ca²⁺	0.623	0.297
A3-Li⁺	0.289	0.060	C3a-Li⁺	0.350	0.103
A3-Na⁺	0.166	0.025	C3a-Na⁺	0.206	0.055
A3-K⁺	0.128	0.031	C3a-K⁺	0.168	0.049
A3-Be²⁺	1.239	0.620	C3a-Be²⁺	1.297	0.653
A3-Mg²⁺	0.723	0.208	C3a-Mg²⁺	0.786	0.274
A3-Ca²⁺	0.591	0.272	C3a-Ca²⁺	0.655	0.320
B1-Li⁺	0.379	0.109	C3b-Li⁺	0.353	0.095
B1-Na⁺	0.229	0.046	C3b-Na⁺	0.206	0.042
B1-K⁺	0.172	0.041	C3b-K⁺	0.158	0.040
B1-Be²⁺	1.322	0.704	C3b-Be²⁺	1.297	0.678
B1-Mg²⁺	0.769	0.266	C3b-Mg²⁺	0.767	0.260
B1-Ca²⁺	0.604	0.252	C3b-Ca²⁺	0.619	0.280

Calculations were performed using B3LYP/6-311+G(2d,2p) optimized geometries

**Fig. 7** Extent of electron charge transfer (q_{CT} , e^-) from aromatic moiety to metal ions based on Mulliken (a), NPA charges (b), calculated at the B3LYP/6-311G(d,p) level

complexes, respectively. Conversely, this trend is reversed when the alkaline earth metals are being considered. Extent of charge transfer values reveals that significant electron charge transfer takes place from ligand to metal ion in all the complexes. The present paper demonstrates how structural modifications of benzene (π -electron source) by ring fusion with monocyclic ring or bicyclic ring or both influence the strength of cation– π interactions.

Acknowledgments We thank the support of the NSF CREST Interdisciplinary Center for Nanotoxicity, Grant # HRD-0833178; NSF-EPSCoR Award #: 362492-190200-01\NSFEPS-0903787. We acknowledge Prof. F. Weinhold for discussion on NPA charges. Mississippi Center for Supercomputing Research (MCSR) is acknowledged for generous computational facilities. We also thank Department of Defense (DoD) High Performance Computing Modernization Program (HPCMP) and ONR for providing computational facilities through ERDC.

References

1. Frontera A, Quiñero D, Deyà PM (2011) WIREs Comput Mol Sci 1:440
2. Schneider HJ (2009) Angew Chem Int Ed 48:3924
3. Reddy AS, Sastry GM, Sastry GN (2007) Prot Struct Funct Bioinf 67:1179
4. Mitchell JB, Nandi CL, McDonald IK, Thornton JM, Price SL (1994) J Mol Biol 239:315
5. Stauffer DA, Karlin A (1994) Biochemistry 33:6840
6. Wintjens R, Liévin J, Rooman M, Buisine E (2000) J Mol Biol 302:395
7. Pletneva EV, Laederach AT, Fulton DB, Kostic NM (2001) J Am Chem Soc 123:6232
8. Dougherty DA (2008) J Org Chem 73:3667
9. Zhong W, Gallivan JP, Zhang Y, Li L, Lester HA, Dougherty DA (1998) Proc Natl Acad Sci USA 95:12088
10. Choi HS, Suh SB, Cho SJ, Kim KS (1998) Proc Natl Acad Sci USA 95:12094
11. Kim D, Hu S, Tarakeshwar P, Kim KS, Lisy JM (2003) J Phys Chem A 107:1228
12. Feller D, Dixon DA, Nicholas JB (2000) J Phys Chem A 104:11414
13. Feller D (2000) Chem Phys Lett 322:543
14. Reddy AS, Sastry GN (2005) J Phys Chem A 109:8893
15. Tsuzuki S, Uchimaru T, Mikami M (2003) J Phys Chem A 107:10414
16. Dinadayalane TC, Hassan A, Leszczynski J (2010) J Mol Struct 976:320
17. Dinadayalane TC, Afanasiev D, Leszczynski J (2008) J Phys Chem A 112:7916
18. Hassan A, Dinadayalane TC, Leszczynski J (2007) Chem Phys Lett 443:205
19. Dinadayalane TC, Leszczynski J (2009) J Chem Phys 130:081101
20. Dinadayalane TC, Leszczynski J (2009) Struct Chem 20:11
21. Dinadayalane TC, Gorb L, Simeon T, Dodziuk H (2007) Int J Quantum Chem 107:2204
22. Dinadayalane TC, Gorb L, Dodziuk H, Leszczynski J (2005) AIP Conf Proc 786:436
23. Wheeler SE, Houk KN (2009) J Am Chem Soc 131:3126
24. Umadevi D, Sastry GN (2011) J Phys Chem C 115:9656
25. Amunugama R, Rodgers MT (2003) Int J Mass Spectrom 227:339
26. Koyanagi GK, Bohme DK (2003) Int J Mass Spectrom 227:563
27. Hunter CA, Low CMR, Rotger C, Vinter JG, Zonta C (2002) Proc Natl Acad Sci USA 99:4873
28. Suresh CH, Gadre SR (2007) J Phys Chem A 111:710
29. McMahon TB, Ohanessian G (2000) Chem Eur J 6:2931
30. Armentrout PB, Rodgers MT (2000) J Phys Chem A 104:2238
31. Kumpf RA, Dougherty DA (1993) Science 261:1708
32. Mecozzi S, West AP Jr, Dougherty DA (1996) J Am Chem Soc 118:2307
33. Dougherty DA (1996) Science 271:163
34. Ma JC, Dougherty DA (1997) Chem Rev 97:1303
35. Gallivan JP, Dougherty DA (1999) Proc Natl Acad Sci USA 96:9459
36. Zacharias N, Dougherty DA (2002) Trends Pharmacol Sci 23:281
37. Gal J-F, Maria P-C, Decouzon M, Mó O, Yáñez M, Abboud JLM (2003) J Am Chem Soc 125:10394
38. Amunugama R, Rodgers MT (2003) Int J Mass Spectrom 227:1
39. Vijay D, Sastry GN (2008) Phys Chem Chem Phys 10:582
40. Vijay D, Sastry GN (2010) Chem Phys Lett 485:235
41. Reddy AS, Vijay D, Sastry GM, Sastry GN (2006) J Phys Chem B 110:2479
42. Reddy AS, Vijay D, Sastry GM, Sastry GN (2006) J Phys Chem B 110:10206
43. Vijay D, Zipse H, Sastry GN (2008) J Phys Chem B 112:8863
44. Escudero D, Frontera A, Quiñero D, Deyà PM (2008) Chem Phys Lett 456:257
45. Estarellas C, Frontera A, Quiñero D, Deyà PM (2009) Chem Phys Lett 479:316
46. Alkorta I, Blanco F, Deyà PM, Elguero J, Estarellas C, Frontera A, Quiñero D (2010) Theor Chem Acc 126:1
47. Macias AT, Norton JE, Evanseck JD (2003) J Am Chem Soc 125:2351
48. Siegel JS (1994) Angew Chem Int Ed Engl 33:1721
49. Frank NL, Baldrige KK, Gantzel P, Siegel JS (1995) Tetrahedron Lett 36:4389
50. Frank NL, Baldrige KK, Siegel JS (1995) J Am Chem Soc 117:2102
51. Bürgi H-B, Baldrige KK, Hardcastle K, Frank NL, Gantzel P, Siegel JS, Ziller J (1995) Angew Chem Int Ed Engl 34:1454
52. Higashibayashi S, Reza AFGM, Sakurai H (2010) J Org Chem 75:4626
53. Fabris F, Pellizzaro L, Zonta C, De Lucchi O (2007) Eur J Org Chem, p 283
54. Zonta C, Fabris F, De Lucchi O (2005) Org Lett 7:1003
55. Dinadayalane TC, Deepa S, Reddy AS, Sastry GN (2004) J Org Chem 69:8111
56. Dinadayalane TC, Deepa S, Sastry GN (2003) Tetrahedron Lett 44:4527
57. Dinadayalane TC, Sastry GN (2002) J Org Chem 67:4605
58. Dinadayalane TC, Priyakumar UD, Sastry GN (2001) J Mol Struct 543:1
59. Carrazana-García JA, Rodríguez-Otero J, Cabaleiro-Lago EM (2011) J Phys Chem B 115:2774
60. Green JR, Dunbar RC (2011) J Phys Chem A 115:4968
61. Engerer LK, Hanusa TP (2011) J Org Chem 76:42
62. Becke AD (1988) Phys Rev A 38:3098
63. Lee C, Yang W, Parr RG (1988) Phys Rev B 37:785
64. Møller C, Plesset MS (1934) Phys Rev 46:618
65. Boys SF, Bernardi F (1970) Mol Phys 19:553
66. Weinhold F personal communication
67. IOP keyword was suggested by Gaussian Help Desk
68. Glendening ED, Reed AE, Carpenter JE, Weinhold F (1998) NBO, Version 3.1. Theoretical Chemistry Institute, University of Wisconsin, Madison, WI

69. Frisch MJ, Trucks GW, Schlegel HB, Scuseria GE, Robb MA, Cheeseman JR, Scalmani G, Barone V, Mennucci B, Petersson GA, Nakatsuji H, Caricato M, Li X, Hratchian HP, Izmaylov AF, Bloino J, Zheng G, Sonnenberg L, Hada M, Ehara M, Toyota K, Fukuda R, Hasegawa J, Ishida M, Nakajima T, Honda Y, Kitao O, Nakai H, Vreven T, Montgomery Jr. JA, Peralta JE, Ogliaro F, Bearpark M, Heyd JJ, Brothers E, Kudin KN, Staroverov VN, Kobayashi R, Normand J, Raghavachari K, Rendell A, Burant JC, Iyengar SS, Tomasi J, Cossi M, Rega N, Millam JM, Klene M, Knox JE, Cross JB, Bakken V, Adamo C, Jaramillo J, Gomperts R, Stratmann RE, Yazyev O, Austin AJ, Cammi R, Pomelli C, Ochterski JW, Martin RL, Morokuma K, Zakrzewski VG, Voth GA, Salvador P, Dannenberg JJ, Dapprich S, Daniels AD, Farkas O, Foresman JB, Ortiz JV, Cioslowski J, Fox DJ (2009) Gaussian 09, revision A.1. Gaussian, Inc, Wallingford
70. Dennington II R, Keith R, Millam T, Eppinnett J, Hovell K, Gilliland WL (2003) GaussView, Version 3.0. Semichem, Inc., Shawnee Mission, KS
71. Aihara J, Ishida T (2010) *J Phys Chem A* 114:1093
72. Stanger A (2008) *J Phys Chem A* 112:12849
73. Mishra BK, Bajpai VK, Ramanathan V, Gadre SR, Sathyamurthy N (2008) *Mol Phys* 106:1557
74. Pauling L (1960) *The nature of the chemical bond*, 3rd edn. Cornell University Press, Ithaca
75. Amicangelo JC, Armentrout PB (2000) *J Phys Chem A* 104:11420
76. Zhu W, Tan X, Shen J, Luo X, Cheng F, Puah CM, Ji R, Chen K, Jiang H (2003) *J Phys Chem A* 107:2296
77. Cheng J, Zhu W, Tang Y, Xu Y, Li Z, Chen K, Jiang H (2006) *Chem Phys Lett* 422:455